

PURDUE UNIVERSITY
SCHOOL OF AERONAUTICS AND ASTRONAUTICS

1N-16398

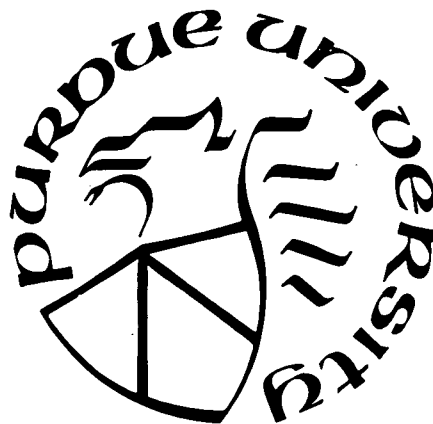
(NASA-CR-177086) THE INTEGRATED MANUAL AND
AUTOMATIC CONTROL OF COMPLEX FLIGHT SYSTEMS
Status Report, Apr. 1985 - Jun. 1986 (Purdue
Univ.) 27 p

N86-28952

CSSL 01C

Unclas

G3/08 43228



West Lafayette, Indiana 47907

AS P 9391092
=

THE INTEGRATED
MANUAL AND AUTOMATIC CONTROL
OF COMPLEX FLIGHT SYSTEMS

Status Report

April, 1985 - June, 1986

Principal Investigator: Dr. David K. Schmidt ✓
School of Aeronautics & Astronautics
Purdue University
West Lafayette, IN 47907

NASA Technical Officer: Mr. Donald T. Berry
Vehicle Dynamics and Control Division
Ames Research Center
Dryden Flight Research Facility
P.O. Box 273
Edwards, CA 93523

Grant No. NAG4-1

July 7, 1986

Table of Contents

	Page
1. Status Summary	1
Appendix A: Closed-Loop, Pilot/Vehicle Analysis of the Approach and Landing Task	3
Appendix B: Cooperative Synthesis of Control and Display Augmentation	13

This constitutes a status report on the research being performed by Purdue University's School of Aeronautics and Astronautics for NASA Ames/Dryden, under grant number NAG4-1. The topics of research in this program include pilot/vehicle analysis techniques, identification of pilot dynamics, and control and display synthesis techniques for optimizing aircraft handling qualities. The project activities for the period of April, 1985 through June, 1986 will be discussed herein.

The following grant-related publications have appeared in the archive journals, and were presented at technical conferences during the reporting period

1. "Closed-Loop, Pilot/Vehicle Analysis of the Approach and Landing Task" (Copy attached in Appendix; A). This paper was presented at the AIAA Guid. & Cont. Conference in August, 1985. Paper No. 85-1851. It is also soon to appear in the Journal of Guidance, Control, and Dynamics.
2. "Normalized Predictive Deconvolution. A Time Series Algorithm For Modeling Human Operator Dynamics," by Biezad and Schmidt. Journal of Guidance, Control, and Dynamics, Vol. 8, No. 6, Nov.-Dec., 1985.
3. "Cooperative Synthesis of Control and Display Augmentation," (copy attached as Appendix B). This paper will be presented at the AIAA Guidance and Control Conf. in Aug., 1986.

The current technical activity is directed at extending and validating the active display synthesis procedure, and the pilot/vehicle

analysis of the NLR rate-command flight configurations in the landing task. After evaluation of the NLR data base, attention will turn to developing a pilot/vehicle analysis methodology for the lateral-directional axis.

Appendix A

CLOSED-LOOP, PILOT/VEHICLE ANALYSIS
OF THE APPROACH AND LANDING TASK

ORIGINAL PAGE IS
OF POOR QUALITY

M.R. Anderson*
D.K. Schmidt†

School of Aeronautics and Astronautics
Purdue University
West Lafayette, IN 47907

Abstract

Optimal-control-theoretic modeling and frequency-domain analysis is the methodology proposed to evaluate analytically the handling qualities of higher-order manually controlled dynamic systems. Fundamental to the methodology is evaluating the interplay between pilot workload and closed-loop pilot/vehicle performance and stability robustness. The model-based metric for pilot workload is the required pilot phase compensation. Pilot/vehicle performance and loop stability is then evaluated using frequency-domain techniques. When these techniques were applied to the flight-test data for thirty-two highly-augmented fighter configurations, strong correlation was obtained between the analytical and experimental results.

Introduction

One important tool in handling-qualities research is the application of closed-loop analysis techniques to expose undesirable dynamic characteristics in the combined pilot and vehicle system. The pilot has been frequently characterized by servo-analytic techniques in the frequency domain. One advantage is the results are in a form very useful to, and understood by, the flight control designer. Much of this work was based on a quasi-linear pilot modeling technique developed and reported by McRuer, et al.^[1]

A significant contribution obtained from a similar technique was furnished by Neal and Smith^[2] in 1970. In this work, Neal and Smith were able to correlate Cooper-Harper^[3] subjective pilot ratings with frequency-domain characteristics of the pilot/vehicle system, as modeled, for a precision pitch-attitude-tracking task. A single-loop, servo-analytic pilot modeling approach was used in this work.

However, the frequency-domain pilot model discussed thusfar has been somewhat limited to single-input, single-output systems. Multi-loop models have been implemented using sequential loop closure techniques, with some limited success. The difficulty in the multi-loop case arises in that assumptions are required as to the pilot/vehicle system's loop structure and to the proper form of the pilot's loop compensation. There are also several difficulties in characterizing task constraints in the frequency domain alone (i.e. required bandwidth).

In the early 1970's, Kleinman, Baron, and Levison^[4] put forth a pilot modeling technique based on a time-domain, optimal-control approach. This

approach has the potential to be very adaptable for more complex, multi-loop situations or tasks. However, much of the research based on this pilot modeling technique has been focused at attempts to predict human operator and vehicle time responses or more specifically, statistical performance. Usually, such statistical information is not the most useful to the flight control designer.

Recently, Bacon and Schmidt^[5] presented an integrated optimal-control, frequency-domain (OC/FD) approach for pilot/vehicle analysis of the precision pitch-attitude control task. When applied to the flight test results of Neal and Smith, the optimal-control approach was shown, not only to agree extremely well with the original results presented by Neal and Smith, but also to yield additional information on achievable closed-loop bandwidth in the task. This methodology also provides a quantitative task definition in the time domain. The pitch-attitude-tracking task was still modeled as a single-input, single-output, closed-loop task, as shown in Fig. 1, but the optimal-control approach was used to obtain reasonable analytic estimates of the pilot's adaptable dynamics, $P(s)$, in the pilot/vehicle systems.

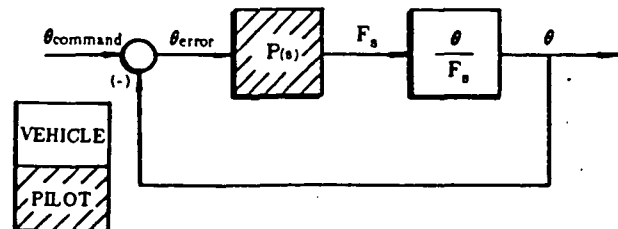


Figure 1 Neal-Smith/Bacon-Schmidt
Pitch Attitude Tracking Task

The research described herein, and in considerable detail in Reference [6], presents an extension of the methodology of Bacon and Schmidt to the more complex approach, flare, and landing task. It is usually understood that this task is multi-loop in nature and the difficulty has been in the estimation of the appropriate pilot loop closures and dynamic compensation. In addition, developing a single model-based metric correlating with workload has been difficult, given multiple pilot loop closures instead of a single, combined pilot/vehicle control loop. The fundamental approach here is to use the time-domain, optimal-control method to estimate the pilot loop closures, and then to perform a frequency-domain analysis which yields a single dynamically-equivalent loop. Finally, the equivalent single loop representation is evaluated to extract pertinent vehicle handling

Copyright © 1985 by M.R. Anderson and D.K. Schmidt.
Published by the American Institute of Aeronautics and
Astronautics, Inc., with permission.

* Graduate Student.

† Professor, Associate Fellow, AIAA.

quality information. The vehicle configurations in consideration here are those initially reported by R.E. Smith^[7] in the LAHOS (Landing and Approach of Higher Order Systems) study. It is again emphasized that what is sought in this analysis is an analytical methodology that will expose unacceptable vehicle dynamics in a piloted task and will at the same time aid in identifying and understanding desired vehicle characteristics.

The Experimental Data Base

The LAHOS report summarizes flight tests conducted using the USAF/Calspan NT-33A variable stability aircraft to study highly augmented fighter aircraft in the landing flight phases under VFR conditions. Several of the configurations were flown with additional control system dynamics described in Table 1. These additional dynamics were used to represent possible control system dynamics which are usually present in highly-augmented aircraft. A summary of the thirty-two configurations selected for study herein is included in Table 2.

Table 1 LAHOS Report Control System Types

Control System Types	
First Order Lag	$\frac{1}{\tau_s s + 1}$
First Order Lead/Lag	$\frac{\tau_l s + 1}{\tau_s s + 1}$
Second Order Lag $\zeta_s = 0.7$	$\frac{1}{\frac{s^2}{\omega_s^2} + 2\frac{\zeta_s}{\omega_s}s + 1}$
Fourth Order Lag, Butterworth Filter to Model Digital Lag $\zeta_s = 0.93, \zeta_4 = 0.38,$ $\omega_s = \omega_4 = 16(\text{rad/sec})$	$\frac{1}{[\frac{s^2}{\omega_s^2} + 2\frac{\zeta_s}{\omega_s}s + 1][\frac{s^2}{\omega_4^2} + 2\frac{\zeta_4}{\omega_4}s + 1]}$

The airframe longitudinal dynamics for the configurations are representable in the standard form

$$\dot{\bar{x}}_v(t) = A_v \bar{x}_v(t) + b_v u(t) \quad (1)$$

where the state vector is defined by, $\bar{x}_v^T = [u, w, \theta, q]$, and the control $u(t)$ is the elevator deflection, $\delta_e(t)$. Using the approximations

$$\gamma(t) = \theta(t) - \frac{1}{U_0} w(t) \quad (2)$$

and

$$\dot{\gamma}(t) = [n_z(t) - 1] g/U_0$$

the vehicle responses of interest may be written

$$\bar{y}(t) = C_v \bar{x}_v(t) + d_v u(t)$$

where

$$\bar{y}^T = [\theta, q, \gamma, n_z] .$$

Table 2 LAHOS Configuration Summary

Aircraft Characteristics				
Config. No.	Aircraft Dyn.	Additional Dyn.		
	$\omega_{sp}(\text{rad/sec})/\zeta_{sp}$	$\tau_1(\text{sec})$	$\tau_2(\text{sec})$	$\omega_s(\text{rad/sec})$
1-C	1.0/0.74	0.2	0.1	-
1-1		-	-	-
1-3		-	0.25	-
1-6		-	-	16
2-A		0.4	0.1	-
2-C	2.3/0.57	0.2	0.1	-
2-1		-	-	-
2-2		-	0.1	-
2-3		-	0.25	-
2-6		-	-	16
2-7		-	-	12
2-9		-	-	6
2-11		-	-	16(4th)
3-C	2.2/0.25	0.2	0.1	-
3-1		-	-	-
3-2		-	0.1	-
3-3		-	0.25	-
3-6		-	-	16
4-C		2.0/1.06	0.2	0.1
4-1	-		-	-
4-4	-		0.5	-
4-6	-		-	16
4-7	-		-	12
4-10	-		-	4
5-1	3.9/0.54	-	-	-
5-3		-	0.25	-
5-4		-	0.5	-
5-5		-	1.0	-
5-6		-	-	16
5-11		-	-	16(4th)
6-1		1.9/0.65	$\frac{16(.5s+1)(.43s+1)}{(.2s+1)(1.1s+1)(s^2+2(.7)s+16)}$	
6-2	$\frac{(.5s+1)(.43s+1)(.06s+1)}{(.2s+1)(1.1s+1)(.1s+1)}$			

As previously mentioned, the different configurations flown for the LAHOS study include a variety of additional control system dynamics. Each of these sets of additional dynamics can be represented by,

$$\dot{\bar{x}}_k(t) = A_k \bar{x}_k(t) + b_k u_p(t)$$

$$u(t) = C_k \bar{x}_k(t) + d_k u_p(t) . \quad (3)$$

where $u_p(t)$ is the stick force applied by the pilot.

Critical Task Modeling

Clearly, for aircraft without direct-lift devices, the ability to control pitch-attitude is necessary in any longitudinal task. But to what extent the pilot has to precisely control attitude such that he can effectively control flight path, for example, is an interesting question to be considered. Here we will attempt to shed some light on this question by performing an attitude analysis as proposed by Bacon and Schmidt. Since that analysis procedure is described in Ref.[5], how it is performed will not be repeated here. However, an additional "critical task analysis" will be developed, and is one which is intended to give additional

information on the vehicle characteristics deemed important in the landing task.

In the approach, flare, and landing task, both altitude and vertical velocity are clearly of critical interest to the pilot. These parameters are both related to the vehicle flight path, which is controllable by the pilot through elevator position commands (in the conventional frontside approach). It is hypothesized, therefore, that the ability to precisely control flight-path-angle is a necessary condition to obtain good pilot ratings for that particular vehicle dynamic configuration in the *approach, flare, and landing task*.

The ability to precisely control flight-path angle, in an analytical sense, is equivalent to the ability to minimize the deviation of flight-path angle from a desired path. A compatible pilot objective, in such a case, may then be stated in the form of a quadratic cost function as used in the optimal-control modeling approach. An appropriate objective function is then,

$$J(u_p) = E \left\{ \lim_{T \rightarrow \infty} \frac{1}{T} \int_0^T (\gamma \gamma_e^2 + r u_p^2 + g \dot{u}_p^2) dt \right\} \quad (4)$$

where

$$\gamma_e = \text{flight path error}$$

and

$$u_p = \text{pilot's control input.}$$

With the pilot's objective defined, attention must be focused on what observations are available to the pilot in the landing task. It is generally accepted that pitch-attitude information is very important in any longitudinal tracking task. For a VFR task as tested in the experiment, vehicle responses available to, or sensed by the pilot are pitch attitude, pitch rate, and plunge acceleration. Also, vehicle speed, or sink rate is observable. Due to the kinematic relationship among these variables, it may reasonably be assumed that the pilot could close control loops based on θ and $\dot{\theta}$ as well as γ and $\dot{\gamma}$ information. Finally, deviation from some desired flight path would be important, and "sensed" somehow, at least internal to the pilot himself.

To complete the critical task definition, some appropriate characterization of the commanded flight-path to be tracked, $\gamma_c(t)$, is necessary. Note that with regard to the precision tracking performance of the closed-loop pilot/vehicle system, it makes little difference whether the desired flight path is internally generated by the pilot, or is some external exogenous command like a flight director, for example. The important consideration in meeting our analysis objectives is not to actually model a desired glide path, but to adequately and consistently represent command signal frequency content that is important to the pilot in the landing task.

With this in mind, a pre-filter driven by "white" noise is used to generate a random pitch-attitude signal with frequency content similar to that in the original discrete instrument pitch-tracking task used by Neal and Smith. This signal is not displayed to the pilot, but is used to generate a commanded flight path using the vehicle's γ/θ response relationship.

$$\frac{\gamma_c(s)}{\theta_c(s)} = \frac{1}{\tau_{p2}s + 1} \quad (5)$$

A value of $1/\tau_{p2} = 0.5 \text{ sec}^{-1}$ was chosen here. In a state-space representation, the command signals are then expressible as

$$\begin{bmatrix} \dot{\theta}_c \\ \dot{\theta}_c \\ \dot{\gamma}_c \end{bmatrix} = \begin{bmatrix} 0 & 1 & 0 \\ -0.25 & -0.5 & 0 \\ 0.5 & 0 & -0.5 \end{bmatrix} \begin{bmatrix} \theta_c \\ \dot{\theta}_c \\ \gamma_c \end{bmatrix} + \begin{bmatrix} 0 \\ 0.25 \\ 0 \end{bmatrix} w$$

or

$$\dot{\bar{x}}_c(t) = A_c \bar{x}_c(t) + e_c w(t) \quad (6)$$

where w is a zero mean, Gaussian white noise process.

Aggregating the command, vehicle, and control system dynamics into one state space representation gives,

$$\begin{bmatrix} \dot{\bar{x}}_c \\ \dot{\bar{x}}_v \\ \dot{\bar{x}}_k \end{bmatrix} = \begin{bmatrix} A_c & 0 & 0 \\ 0 & A_v & b_v C_k \\ 0 & 0 & A_k \end{bmatrix} \begin{bmatrix} \bar{x}_c \\ \bar{x}_v \\ \bar{x}_k \end{bmatrix} + \begin{bmatrix} 0 \\ b_v d_k \\ b_k \end{bmatrix} u_p + \begin{bmatrix} e_c \\ 0 \\ 0 \end{bmatrix} w$$

$$\bar{y}_p = [C_c \ C_v \ d_v C_k] \begin{bmatrix} \bar{x}_c \\ \bar{x}_v \\ \bar{x}_k \end{bmatrix} + [d_v d_k] u_p + v \quad (7)$$

The command/vehicle system is now in the desired form,

$$\dot{\bar{x}}(t) = A \bar{x}(t) + b u_p(t) + e w(t)$$

$$\bar{y}_p(t) = C \bar{x}(t) + d u_p(t) + v(t) \quad (8)$$

with obvious definitions for A , b , e , C , and d . Finally, the pilot's observation vector, y_p is given by

$$y_p^T = [\gamma_e, \dot{\gamma}_e, \gamma, \dot{\gamma}, \theta, \dot{\theta}] \quad (9)$$

where

$$\gamma_e = \gamma_c - \gamma$$

These observations lead to the block diagram description of the pilot/vehicle system shown in Fig. 2. Here the cross-hatched blocks represent pilot compensation in his control loops.

More detailed development and description of the methodology can be found in References [5] and [6]. It will only be necessary to outline a few pertinent points here. The optimal control model uses the time-domain description of the pilot's sensing and response limitations. Statistical representation of these limitations, relevant to this report, are summarized in Table 3. The values of τ , the pilot's observation delay, and τ_n , the pilot's neuromuscular lag time constant, are chosen to represent the human operator in his most aggressive mode. This is done, coincident with our analysis objectives, to expose handling quality "cliffs" in the flight configurations by modeling the pilot's most aggressive control techniques.

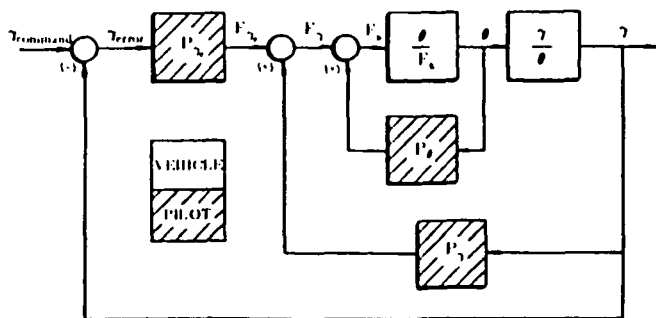


Figure 2 The Multi-Loop Flight Path Tracking Task

Table 3 Pilot Model Parameters

Pilot Model Parameters	
Parameter	Value
Observation Vector	$\bar{y}_p^T = [\gamma_e, \gamma_e, \gamma_e, \theta, \theta]$
Objective Function Weights	$q_n = [16, 0, 0, 0, 0]$ $r_{F_s} = 0$
Observation Thresholds	$T_{\gamma_e, \gamma_e} = 0.05 \text{ deg}$ $T_{\theta, \theta} = 0.18 \text{ deg/sec}$
Observation Noise Ratio	-20 dB All Observed Variables
Fractional Attention	$f_1 = 0.3333$ All Observed Variables
Observation Delay	$\tau = 0.2 \text{ sec}$
Neuromuscular Lag	$\tau_n = 0.1 \text{ sec}$
Motor Noise Variance	-25 dB
Control Input	F_s (Stick Force in lbs.)

The coherent part of the pilot's control response can be described in terms of a pilot transfer matrix defined by,

$$u_p(s) = H(s)\bar{y}_p(s) \quad (10)$$

The pilot transfer matrix is obtained directly from the optimal control approach solution,

$$H(s) = \frac{-l_e}{\tau_n s + 1} \left\{ (sI - \hat{A}) \int_0^{\tau} e^{(sI - \hat{A})\sigma} d\sigma (sI - A_1 + b_1 l_e) + sI - \hat{A} + b_1 l_e \right\}^{-1} \Sigma_1 C_1^T V^{-1} \quad (11)$$

with

$$l_e = [K \ 0],$$

$$A_1 = \begin{bmatrix} A & b \\ 0 & -1/\tau_n \end{bmatrix},$$

$$b_1 = \begin{bmatrix} 0 \\ 1/\tau_n \end{bmatrix}.$$

$$C_1 = [C \ d].$$

Also, the \hat{A} matrix is derived from a Kalman state estimator,

$$\hat{A} = A_1 - \Sigma_1 C_1^T V^{-1} C_1$$

where Σ_1 is the steady state error covariance and V is the pilot's observation noise intensity.

For the critical task as modeled, the pilot control input can be expanded in terms of the pilot's transfer function matrix and pilot observations,

$$u_p(s) = [H_{\gamma_e}(s) + sH_{\dot{\gamma}_e}(s)]\gamma_e(s) + [H_{\gamma_e}(s) + sH_{\dot{\gamma}_e}(s)]\gamma(s) + [H_{\theta}(s) + sH_{\dot{\theta}}(s)]\theta(s) \quad (12)$$

where, for example, the Laplace Transform definition

$$L\{\dot{\theta}(t)\} = s\theta(s)$$

has been used for the angular rates. An effective pilot transfer function, associated with any pilot observation η , can now be defined by,

$$P_{\eta}(s) = H_{\eta}(s) + sH_{\dot{\eta}}(s)$$

so that the pilot's control input becomes a linear combination of effective pilot transfer functions and observations,

$$u_p(s) = P_{\gamma_e}(s)\gamma_e(s) + P_{\gamma}(s)\gamma(s) + P_{\theta}(s)\theta(s) \quad (13)$$

The pilot control input above is, of course, perfectly compatible with the block diagram representation of the flight-path-tracking task previously introduced (see Fig. 2). An example of the effective pilot frequency responses are shown in Fig. 3 for LAHOS Configuration 2-2. With the frequency responses of the effective pilot transfer functions now available, discussion will turn to closed-loop analysis of the handling characteristics of the LAHOS configurations.

Analysis and Results

The actual analysis consists first of an evaluation of the attitude dynamics alone, using a variation of the Bacon and Schmidt^[6] procedure. The intent being that obviously undesirable attitude dynamics should be exposed at the outset. The hypothesis is that for aircraft in which flight-path is controlled by pitch-attitude, some definition and evaluation of the minimum ability to control attitude is necessary even though flight-path control is the ultimate goal. Neal and Smith, as well as Bacon and Schmidt, were able to analyze the pilot/vehicle handling-quality criteria problem in the attitude control task as a trade-off between pilot workload required to achieve acceptable task performance and a subsequent measure of the pilot/vehicle closed-loop performance. Traditionally, pilot workload has been shown to correlate with the pilot's phase equalization required.

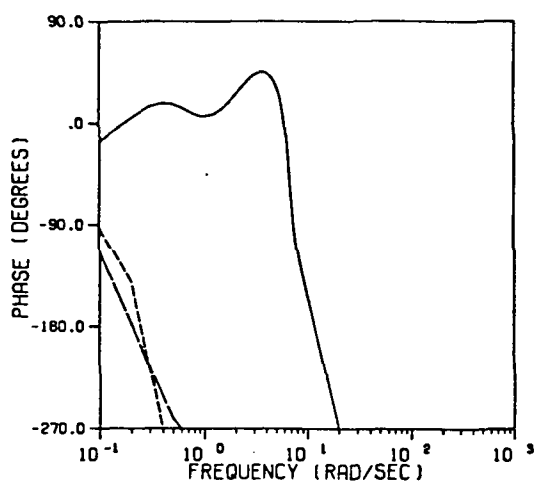
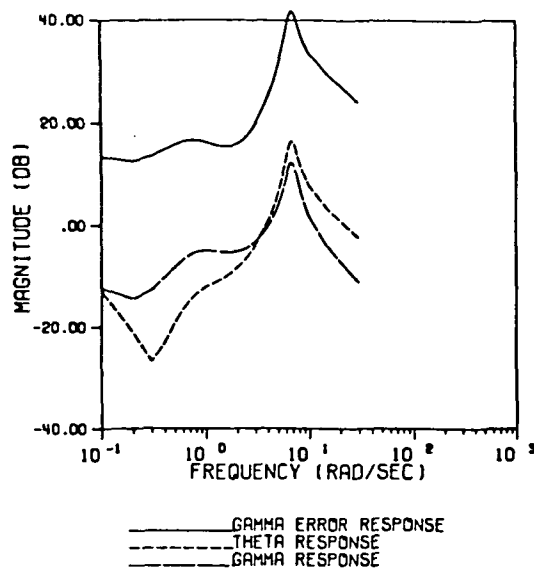


Figure 3 Configuration 2-2 Effective Pilot Transfer Functions

Bacon and Schmidt, as did Neal and Smith, use the pilot's phase compensation, as modeled at their closed-loop bandwidth frequency, to quantify the pilot's task workload in the attitude tracking task. They also used the magnitude of the resonant peak of the closed-loop θ/θ_c frequency response as a gauge of closed-loop performance and stability, in terms of high frequency oscillation tendencies of the pilot/vehicle system. In both analysis procedures, however, some limit was selected on the maximum allowable "low-frequency droop" of the closed-loop frequency response.

More recently, Waszak and Schmidt^[8] have been able to characterize the closed-loop performance of the pilot/vehicle system through the use of a sensitivity parameter defined to evaluate the change in closed-loop resonant peak due to a small change (10%) in the pilot/vehicle forward path gain. This sensitivity parameter, defined by

$$SP = (\text{low frequency droop}) \left| \frac{\Delta \text{ resonant peak}}{\Delta \text{ pilot gain}} \right| \quad (14)$$

gave results indicated in Fig. 4 for the original Neal-Smith pitch-attitude-tracking configurations also evaluated by Bacon and Schmidt^[8].

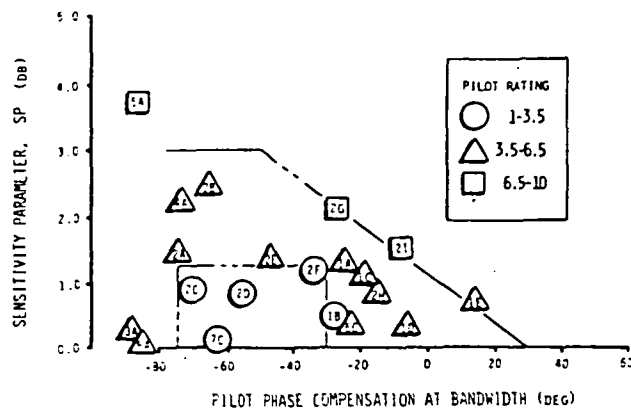


Figure 4 Neal-Smith/Waszak-Schmidt Pitch Attitude Tracking Results

Applying this pitch-attitude-tracking modeling methodology to the LAHOS data set reveals the results shown in Fig. 5. It is obvious from a comparison of Fig. 4 and Fig. 5 that the LAHOS configurations are grouped nicely, in terms of Level 1, 2, and 3 ratings, but with higher pilot phase compensation required in the LAHOS data set (landing task) as compared to the Neal-Smith configurations (attitude tracking task). This difference is of course consistent with lower short-period frequencies corresponding to the lower airspeeds encountered in the landing task, thereby requiring the pilot to generate more phase lead in landing than in an up-and-away flight condition. However, by the placement of the pilot-rated Level 1 region in Fig. 5, one can conclude that the pilot actually accepts the required generation of a modest amount of phase lead in the landing task, while the same phase lead requirement would result in a Level 2 rating in a pure attitude tracking task. It is clear, therefore, that although the ratings of the configurations in the landing task correlate well with the resonance peak sensitivity and phase compensation, the Neal-Smith criteria cannot be applied directly to infer or predict ratings in the landing task. Adjustments in the allowable phase compensation and peak sensitivity (or peak) consistent with the results of Fig. 5 is suggested.

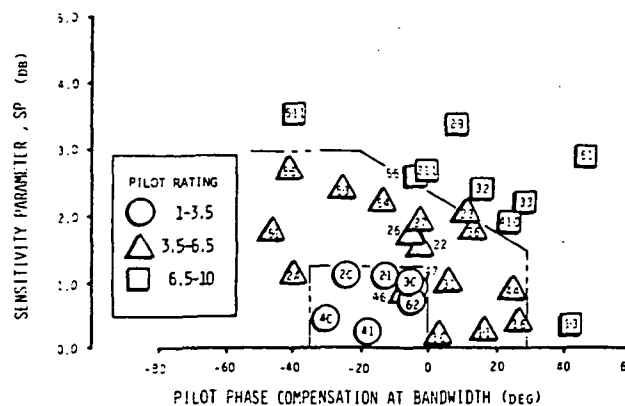


Figure 5 LAHOS Configurations Pitch Attitude Tracking Results

Attention is now turned toward the analysis of the LAHOS data base in the critical flight-path tracking task. In this task, however, directly identifying the pilot's phase compensation is not easily accomplished with the current multi-loop block diagram arrangement. However, the block diagram in Fig. 2 can be manipulated, using the results from Fig. 3, for example, to give an equivalent, single-loop representation of the flight-path-tracking task by defining,

$$P_{eq}(s) = P_{\gamma}(s)G_{\theta}(s)G_{\gamma}(s) \quad (15)$$

where

$$G_{\theta}(s) = \frac{1}{1 - P_{\theta}(s) \left[\frac{\theta}{F_s}(s) \right]}$$

and

$$G_{\gamma}(s) = \frac{1}{1 - P_{\gamma}(s)G_{\theta}(s) \left[\frac{\gamma}{F_s}(s) \right]}$$

This equivalent form is now as shown in Fig. 6.

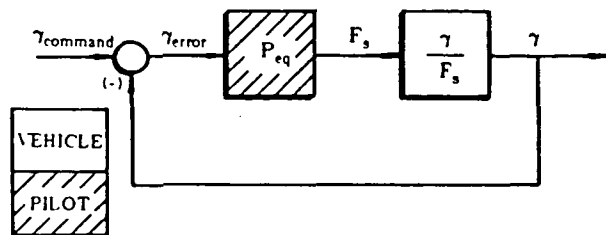


Figure 6 Flight Path Tracking with Equivalent Pilot Function

Fig. 7 illustrates the equivalent single-loop pilot function for LAHOS Configuration 2-2, obtained from the vehicle dynamics and from the data in Fig. 3. From this figure, one can readily see that the pilot is again required to generate lead in the flight-path-tracking task, in order to stabilize and maximize the tracking performance of the closed-loop, pilot/vehicle system. The lead generated (maximum equivalent phase peak) is then suggested as a model-based indication of pilot workload.

Bacon and Schmidt also advanced the use of required closed-loop bandwidth as an indicator of the combined pilot/vehicle system's ability to track over the frequency band. Bandwidth is defined here, as per Neal and Smith, as the frequency at which the closed-loop phase equals -90 degrees. The closed-loop bandwidth, determined from the combined pilot/vehicle system, depends, of course, upon both the vehicle and pilot dynamics (particularly the neuromotor lag time constant, τ_n). As the pilot model parameters have been held constant for all configurations studied, and the smallest achievable τ_n has been assumed, insufficient bandwidth is directly related to sluggish vehicle response. Results shown in Fig. 8 verify that low comparative bandwidth correlates with higher (worse) pilot ratings. However, once sufficient bandwidth is attained, other methods must be applied to uncover handling quality deficiencies.

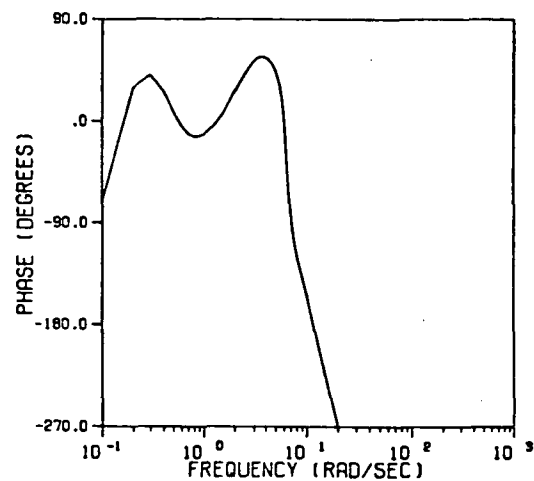
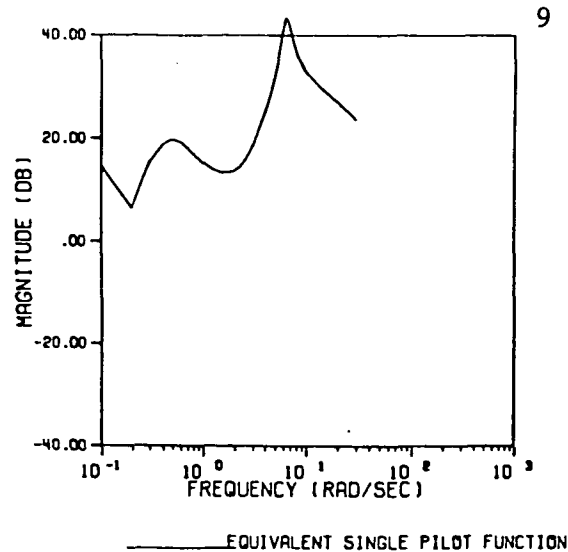


Figure 7 Configuration 2-2 Equivalent Single Loop Pilot Function

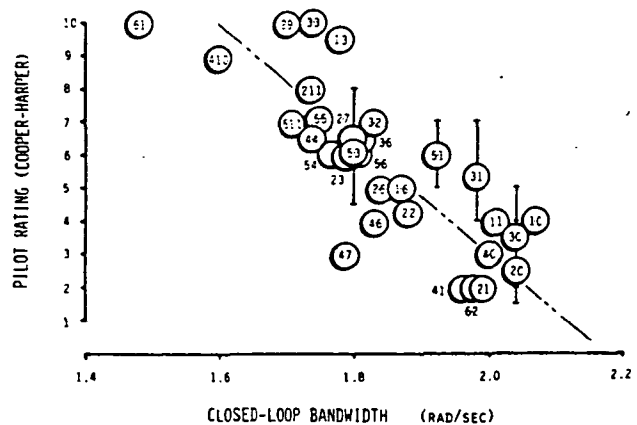


Figure 8 Pilot Rating and Bandwidth Correlation

One of the most important aspects of closed-loop performance is the stability robustness of the loop itself. Stability robustness, here interpreted as insensitivity to small changes in pilot compensation, can best be measured using the combined pilot/vehicle open-loop Bode, or frequency response. Fig. 9, for example, shows the open- and closed-loop frequency responses for LAHOS Configuration 2-2.

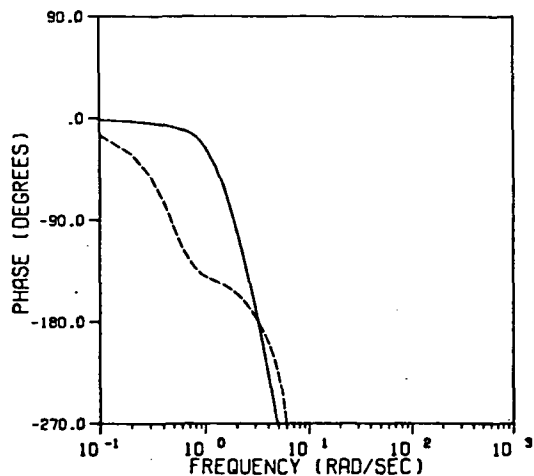
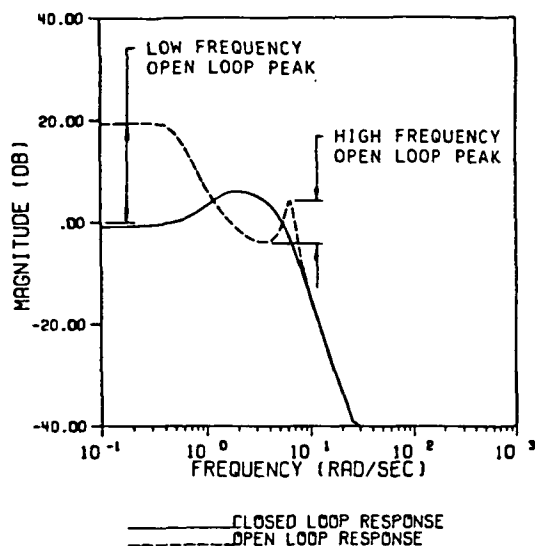


Figure 9 Configuration 2-2 Open and Closed Loop Frequency Responses

For good closed-loop stability margins in a tracking system, the desired "shape" of the open-loop frequency response in the crossover region is well known (i.e., constant slope of -20 dB/decade). Any deviation from the desirable frequency response could then be thought of as a reduction in loop quality or performance. From Fig. 9, one can see a large peak evident in the open-loop frequency response at a frequency just greater than the crossover frequency. A Nyquist diagram of the same open-loop response (see Fig. 10) illustrates that any small phase or gain change injected by the pilot could cause an instability in this system. The magnitude of this peak as defined in Fig. 9, herein entitled the *high-frequency open-loop peak* is

therefore a measure of loop performance, due to its close association with loop stability robustness properties. Also shown for comparison in Fig. 10 is the Nyquist contour for Configuration 2-1, which received a better rating in the task.

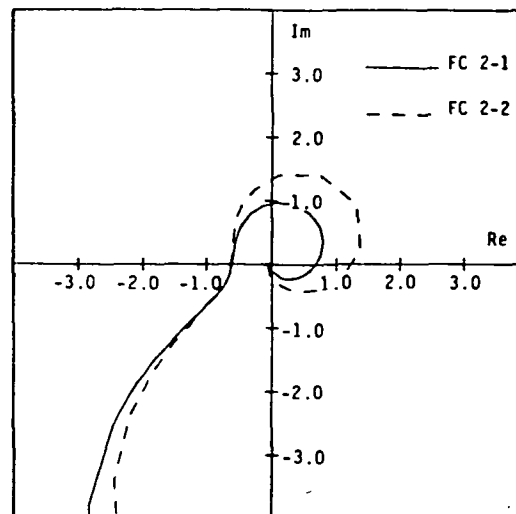


Figure 10 Nyquist Diagram for Configurations 2-1 and 2-2

The genesis of this peak is significant too. Fig. 11 shows the frequency response of the LAHOS Configuration 2-2 flight-path to stick-force transfer function. Considering this figure, and that of the equivalent pilot function shown in Fig. 7, one can readily see that the high frequency open-loop peak in the $\gamma/\gamma_c(s)$ response (in Fig. 9) is due solely to the magnitude distortion arising from the pilot's frequency response. As in any dynamic lead-lag compensator design, magnitude distortion of this type will develop when the compensator is required to achieve significant phase lead. This is easily verified by the large phase-lead peak in the equivalent pilot in Fig. 7. Again, this phase lead has been introduced in the (pilot's) compensation in an effort to maximize the closed-loop bandwidth, and provide stability, within the constraints of the pilot's inherent dynamic limitations.

A plot of the high-frequency open-loop peak versus maximum pilot phase compensation, as in Fig. 12, reveals a characteristic grouping of the vehicle configurations not unlike those of References [2],[5] and [8]. Those configurations rated best overall (Cooper-Harper Level 1) in the *approach and landing task* are appropriately grouped together. The pilot phase compensation results for these vehicle configurations indicate that a certain amount of effective phase lead is acceptable to the pilot in the flight-path-tracking task also. Those configurations rated poorly (Level 2,3) in the approach and landing task would appear to suffer either from insufficient loop quality, as measured by the high-frequency open-loop peak, and/or excessive pilot workload.

An additional evaluation of loop quality stems from the critical task definition - to minimize flight-path error. In fact, the time-domain minimization of error has been used in several past efforts as a loop performance measure (c.f. Refs. 9-12).

This area of performance or loop quality evaluation may also be analyzed in the frequency-domain. Neglecting noise sources, the steady-state, mean-squared flight-path-error may be expressed as,

$$\sigma_{\gamma_e}^2 = \frac{1}{\pi} \int_0^{\infty} \left| \frac{\gamma_e}{\gamma_c} (j\omega) \right|^2 S_{\gamma_c}(\omega) d\omega \quad (16)$$

where $S_{\gamma_c}(\omega)$ is the power spectral density of the commanded input. One can easily see from Eq. (16) above that in order to minimize $\sigma_{\gamma_e}^2$, $\left| \frac{\gamma_e}{\gamma_c} (j\omega) \right|^2$ must be small when $S_{\gamma_c}(\omega)$ is large. This objective forces $\left| \frac{\gamma}{\gamma_e} (j\omega) \right|^2$ to be large ($\left| \frac{\gamma_e}{\gamma} (j\omega) \right|^2 \approx 1$ for a tracking system) at low frequencies. Therefore, the maximum value of the low-frequency pilot/vehicle open-loop frequency response will give an indication, in the frequency-domain, of the tracking performance. This peak value, defined here as the *low-frequency open-loop peak*, can also be plotted along with the previously defined workload metric, as in Fig. 13. Here again, the characteristic grouping of the thirty-two flight configurations is evident, therefore, this low-frequency peak is also offered as an indication of loop quality.

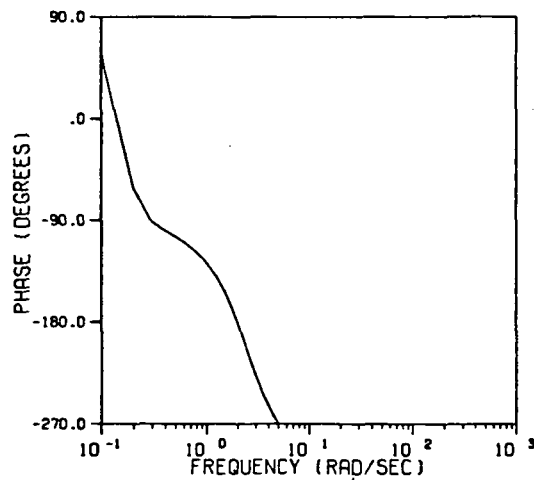
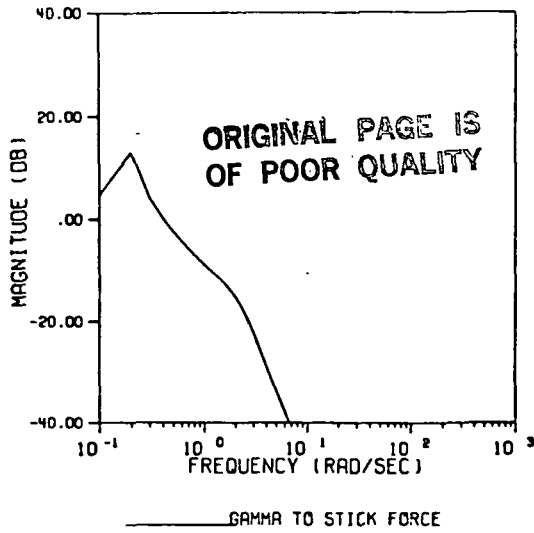


Figure 11 Configuration 2-2 Flight Path to Stick Force Frequency Response

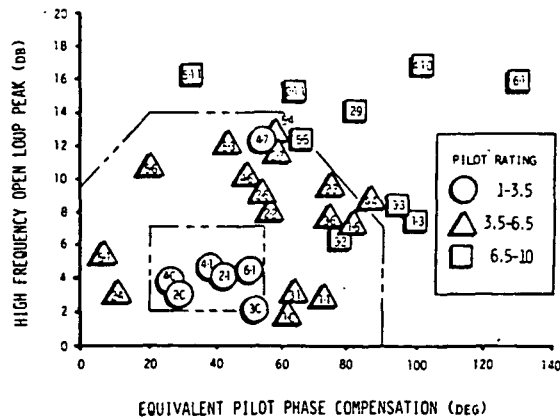


Figure 12 High Frequency Open-Loop Peak Results for the Flight Path Tracking Task

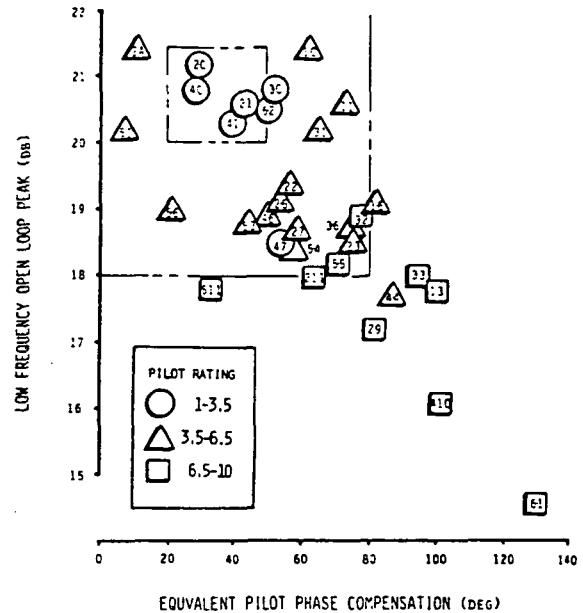


Figure 13 Low Frequency Open-Loop Peak Results for the Flight Path Tracking Task

Conclusion

An optimal-control/frequency-domain (OC/FD) methodology is presented, intended as a dynamic handling-qualities analysis tool appropriate for such complex, multi-loop, man-machine tasks as aircraft approach, flare, and landing. When an analysis of just the pitch-attitude tracking ability was performed on the landing-task data base (LAHOS), a grouping of the configurations similar to the Neal-Smith results was obtained. However, direct application of the Neal-Smith criteria does not appear appropriate for estimating the ratings in the landing task since, among

other things, the pilot appears to accept higher phase compensation requirements in the landing task. The proposed technique for such an attitude analysis is a variation of the method of Bacon and Schmidt that does not require any selection of closed-loop "droop" nor closed-loop bandwidth to perform the analysis.

A critical flight-path control task was developed, and when a closed-loop analysis of this task was performed using the LAHOS data base, excellent correlation was obtained with several model-based quantities of engineering significance. First, correlation was evident between the ratings of the configurations in the landing task and the closed-loop bandwidth obtained from closed loop analysis of the critical task. Also, strong correlation was noted between the ratings and the pilot phase compensation, as modeled, and two measures of loop quality proposed, all of which result from the closed-loop analysis technique. The pilot phase compensation associated with a single analytically obtained describing function, dynamically equivalent to the multi-loop model, was suggested as a workload metric. A low-frequency open-loop peak, related to the ability to minimize flight path deviations, and a high-frequency open-loop peak, indicating insufficient stability robustness properties, were recommended as measures of loop performance. Finally, the quantities used in the analysis technique are fundamental in linear systems analysis, and are aimed at providing significant insight into the causes of, and remedies for unacceptable man-machine system characteristics.

Acknowledgement

This work has been sponsored by the NASA Dryden Flight Research Facility/Ames Research Center under Grant NAG4-1. Mr. Donald T. Berry is the technical monitor. This support is gratefully appreciated.

Also, a significant portion of the software development, and early conceptual ideas were due to Mr. Dan Garrett while a graduate student in the School of Aeronautics and Astronautics. Mr. Garrett is now with McDonnell Aircraft Co., St. Louis.

References

- [1] McRuer, D., Grabam, D., Krendel, E., Reisener, W. Jr., "Human Pilot Dynamics in Compensatory Systems," Flight Dynamics Laboratory, WPAFB, Ohio, AFFDL-TR-65-15, July 1965.
- [2] Neal, T.P. and Smith, R.E., "An In-Flight Investigation to Develop System Design Criteria for Fighter Airplanes," Vol. I, Flight Dynamics Laboratory, WPAFB, Ohio, AFFDL-TR-70-74, Dec. 1970.
- [3] Cooper, G.E. and Harper, R.P. Jr., "The Use of Pilot Rating in Evaluation of Aircraft Handling Qualities," NASA TND-5153, 1969.
- [4] Kleinman, D.L., Baron, S., and Levison, W.H., "An Optimal Control Model of Human Response, Pt. I & II," *Automatica*, Vol. 6, May 1970, pp. 357-383.
- [5] Bacon, B.J. and Schmidt, D.K., "An Optimal Control Approach to Pilot/Vehicle Analysis and the Neal-Smith Criteria," *Journal of Guidance and Control*, Vol. 6, Sept.-Oct. 1983, pp. 339-347.
- [6] Anderson, M.R., "Closed-Loop, Pilot/Vehicle Analysis of Approach and Landing," M.S. Thesis, Purdue University, December 1984.
- [7] Smith, R.E., "Effects of Control System Dynamics on Fighter Approach and Landing Longitudinal Flying Qualities," Flight Dynamics Laboratory, WPAFB, Ohio, AFFDL-TR-78-122, March 1978.
- [8] Waszak, M.R., "Analysis of Flexible Aircraft Longitudinal Dynamics and Handling Qualities," M.S. Thesis, Purdue University, May 1984.
- [9] McDonnell, J.D., "Pilot Rating Technique for the Estimation and Evaluation of Handling Qualities," Flight Dynamics Laboratory, WPAFB, Ohio, AFFDL-TR-68-76, 1968.
- [10] Anderson, R.O., "A New Approach to the Specifications and Evaluation of Flying Qualities," Flight Dynamics Laboratory, WPAFB, Ohio, AFFDL-TR-69-120, 1970.
- [11] Hess, R.A., "Prediction of Pilot Opinion Ratings Using an Optimal Pilot Model," *Human Factors*, Vol. 19, Oct. 1977, pp. 459-475.
- [12] Schmidt, D.K., "On the Use of the OCM's Objective Function as a Pilot Rating Metric," *Proceedings of the 17th Annual Conference on Manual Control*, Los Angeles, CA, June 1981.

Appendix B

ORIGINAL PAGE IS
OF POOR QUALITYSanjay Garg *
D.K. Schmidt **
School of Aeronautics and Astronautics
Purdue University
West Lafayette, IN 47907ABSTRACT

The Cooperative Control Synthesis (CCS), previously developed to synthesize control augmentation so as to optimize pilot opinion rating, is extended to the synthesis of display augmentation for closed-loop manual control tasks. The procedure allows simultaneous solution for the display augmentation and control augmentation gains using optimal-control techniques, and explicitly includes task related and pilot-centered requirements in the design objectives. Use of the methodology is demonstrated by considering a compensatory tracking task and k/s^2 controlled element dynamics. Analytical evaluation of the various control and display augmentation designs synthesized using the cooperative methodology indicates that simultaneous synthesis may lead to a better control display trade-off, as opposed to designing the display after the control augmentation has already been designed.

I. INTRODUCTION

With the advent of high performance aircraft, the amount of information to be processed by the pilot to successfully accomplish the assigned task has continued to increase. It has, therefore, become more critical to determine the best informational set and display dynamics needed by the pilot so as to reduce the pilot's workload and improve performance. In Ref. [1] it was hypothesized that there exists a trade-off between levels of control augmentation of a plant and display augmentation in terms of pilot workload and task performance. That is, a highly sophisticated display with minimum stability augmentation or a high level of control augmentation with lesser display integration or intermediate combinations thereof will be equally acceptable to the pilot. High degree of sophistication in either displays or controls not only implies higher costs but also the pilot must regress further in case of a failure. The hypothesis of Ref. [1] was borne out by the extensive man-in-the-loop simulation work done by Lebacqz et al. [2,3] in their effort to quantify the display/control requirements for helicopter approach and landing. They reported that there was a display/control trade-off for pilot ratings of satisfactory, while ratings of adequate-but-unsatisfactory depended primarily on the control system. Even with flight directors for all three axes, the pilots found it difficult to fly without adequate flight control augmentation.

Another area where display control trade-offs may be of importance is flight test trajectory control (FTTC). A very high degree of accuracy in following complex trajectories can be achieved by automatic controllers [4], but it is undesirable to take the pilot completely out of the control loop. Trajectory guidance systems have also been shown to lead to discernible improvements in the ease and accuracy with which pilots have approached and maintained the desired flight test conditions or trajectories [5]. A combination of trajectory guidance and control augmentation may then lead to desirable levels of accuracy while still maintaining the pilot in the loop.

Thus there exists a need to synthesize stability augmentation and display augmentation with special attention to the role of the pilot in the system, for a specified task. In this paper, a methodology is presented that is intended to provide a systematic approach to synthesizing pilot-optimal control and display augmentation in complex, closed-loop manual control tasks. This methodology is an extension of the cooperative control synthesis (CCS) technique developed earlier [6,7] for control augmentation synthesis. The characteristic results from the methodology are then investigated by considering a compensatory tracking task beginning with a simple k/s^2 plant. Although the methodology is clearly intended for higher order multi-channel tasks, use of this plant and task is appropriate to gain insight, and for validation studies.

II. BACKGROUND

The idea that a control augmentation system works in cooperation with the pilot, and a technique which considers the augmentation system and the pilot to be two controllers working in "parallel" was suggested by Schmidt [6]. This cooperative control synthesis technique incorporates a mathematical model of the pilot behavior and uses optimal-control theory to synthesize control gains that are pilot-optimal as modelled. Since display augmentation, like control augmentation, has to be in harmony with the pilot's abilities and limitations in order to be acceptable to him as an aid in accomplishing his task, the cooperative synthesis technique was considered to provide an appropriate framework for simultaneously synthesizing control and display augmentation and thus provide a task specific trade-off between control and display augmentation.

In the Appendix, the problem formulation for the extension to the control/display design case is presented in its most general form, and the necessary conditions for optimality are stated.

* Graduate student, student member AIAA

**Professor, Assoc. Fellow AIAA

The details of the derivation can be found in Ref. [8]. The application of the methodology to pilot-in-the-loop synthesis of control and display augmentation will be discussed in Section III.

Other display design techniques based on an optimal control model (OCM) [9] of the pilot have been suggested by Levison [10], Hess [11] and Kleinman et al. [12]. All these techniques are intended to lead to flight director designs that reduce pilot workload, and are clever applications of the OCM. All are iterative in nature and involve designing the flight director law after any control augmentation system has been designed. Therefore, these do not explicitly include the display/control trade-off in the synthesis procedures themselves.

An excellent discussion of the functional requirements for the design of flight directors can be found, for example, in Ref. [13]. In summary, the fundamental control and guidance requirement is to reduce the tracking error to zero in a stable, well damped and rapid manner. The main pilot-centered requirement, whether considering control or display augmentation, is that the effective controlled element as perceived by the pilot be like k/s over a broad frequency region. With such a controlled element, the pilot's compensation is a pure gain, which is optimal from the point of minimum pilot compensation workload. However, not only must the pilot-centered requirements be met, but also good overall closed-loop performance must be obtained. As will be shown, a performance/workload trade-off exists.

Consider a compensatory tracking task with a K_o/s^2 plant as in Fig. 1. As is well known, such a plant is difficult to control in that it requires the pilot to generate lead, which results in deterioration in performance and pilot ratings. Rate feedback can then be used to provide the pilot with lead information, either in the form of a "quickened" display, or changed plant dynamics using control augmentation, or a combination of both as shown in Fig. 2. In Fig. 2, K_d is the display "quickening" gain and K_c is the plant augmentation control gain. A feedforward gain K_δ on the pilot's control input (δ_p) is used to compensate for the reduced control effectiveness of the plant when using feedback control augmentation.

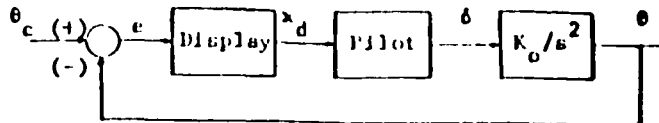


Fig. 1 Compensatory Tracking Task with K_o/s^2 Plant

With display augmentation only, the effective controlled element is :

$$x_d(s)/\delta_p(s) = \frac{K_o(K_d s + 1)}{s^2}$$

Thus the controlled element as seen by the pilot is like k/s for frequencies greater than $1/K_d$. In their extensive experimental work, McRuer et al. [14] found that for a pure k/s like element, the crossover frequency of the piloted system is $\omega \approx 4.3$ rads/sec and the pilot's compensation in the cross-over region is given by $P(s) = K_p e^{-\tau s}$ with $\tau \approx 0.23$ seconds for a command input bandwidth of 1.5 rads/sec. Thus for this display-augmented system to be like k/s at crossover, and be stabilizable by the above form of pilot compensation, we require that the value of K_d be such as to provide a lead of ≈ 57 deg. at crossover. This leads to the requirement that $1/K_d = 2.3$, i.e. $K_d \approx 0.4$. The tracking error is then given by :

$$e(s)/\theta_c(s) = \frac{s(s + K_o K_d P(s))}{(s^2 + K_o K_d P(s)s + K_o P(s))}$$

Thus, for a step command, the error approaches zero in the steady-state, which shows that the rate-augmented display satisfies the control and guidance requirement of Ref. [13]. However, since the pilot is not directly perceiving the error alone, some loss in tracking performance may result.

Conversely, consider control augmentation without an augmented display ($K_d=0$). Now with rate feedback augmenting the plant, the effective controlled element is :

$$\theta(s)/\delta_p(s) = \frac{K_o K_c}{s(s + K_o K_c)}$$

(here $K_c = 1 + K_\delta$ is assumed in Fig. 2). Thus the

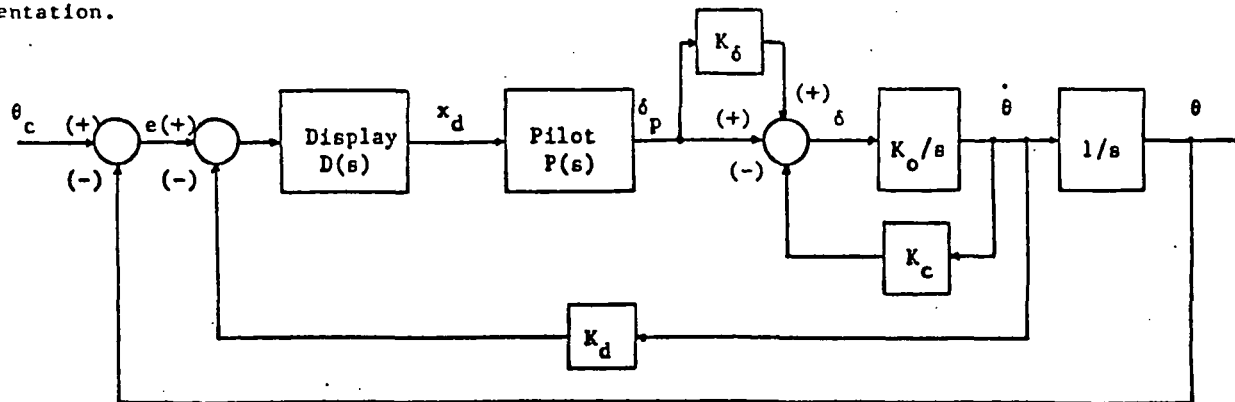


Fig. 2 Display/Control Augmentation using Rate Feedback

controlled element is like k/s for frequencies less than K_c. Using the same argument as before, the requirement on K_c for the system to be stabilizable by a pure gain pilot compensation is K_c > 7.8.

Note that these values of K_d and K_c are desirable primarily from the point of view of minimizing pilot workload. In reality there would be restrictions on allowable values of these gains based on performance requirements and limits on loop bandwidth of the control augmented system. With display augmentation, if K_d becomes too large the tracking error will increase as the pilot would then be making θ̇ (rather than θ) track θ_c.

Even though the objective of both the control augmentation and display augmentation is to aid the pilot, the way this is achieved is fundamentally different for the two types of augmentation as illustrated by the above discussion. In display augmentation, the required lead is provided to the pilot by a change in the numerator dynamics of the effective controlled element, while in control augmentation the denominator is changed, thus affecting the stability properties of the dynamics being controlled by the pilot.

With both control and display augmentation, the effective controlled element is :

$$x_d(s)/\delta_p(s) = \frac{K_c K_d (K_c s + 1)}{s(s + K_c K_d)}$$

Then clearly by letting K_cK_d = 1/K_d, the controlled element can be made like k/s over the whole frequency region. But, as stated earlier, there would be limits imposed on values of K_c and K_d by requirements other than those of just minimizing pilot workload. In this simple example, one is already faced with the question of how to "best" trade-off control and display augmentation.

III. APPLICATION OF COOPERATIVE SYNTHESIS

In the Appendix, a dual performance optimization problem is discussed and the necessary conditions for the optimality of the various controllers, and the expressions for the resulting gain matrices, are derived. The interaction between the various controllers is shown in Fig. A.1. The association of Controller 2 (u₂) with plant augmentation, and of display control (u_d) with the display augmentation should be apparent in this formulation. Moreover, with F₁=0 in (A.11) and u₁=δ̇_p (δ̇_p is the pilot's input) along with appropriate definition of the system matrices A_o and B_{1o}, the structure of the Controller 1 that evolves from the above formulation is similar to that of the Optimal Control Model (OCM) - except for the simplification that the pilot's observation time delay τ has been eliminated in the observations for Controller 1. The elimination of the time delay simplifies the dynamic order of the pilot model by eliminating the linear predictor in the control structure. The pilot's motor noise (v̇) is however accounted for in this formulation in that

it may appear as an additional disturbance in Eqn. (A.1).

It is worth mentioning here that although the simplified pilot model is used in the synthesis procedure presented in this report, the complete model (with predictor, etc.) is used to evaluate candidate designs. Moreover, at each iteration of the synthesis process, the parameters (e.g. noise intensities) in the simplified model are updated to yield results that are consistent with the complete OCM model. It has been shown [15] that by selecting proper noise intensities for the control noise v̇_m and the measurement noise v̇_y, the simplified model may yield the same human operator dynamics as the complete model. In this manner the cooperative methodology, as developed above, can be used to do "pilot in the loop" synthesis of the display/control augmentation design.

IV. AN EXAMPLE

Consider again the simple compensatory tracking task, as in Fig. 1, with the controlled element (plant) dynamics as considered in Ref.[7]:

$$\theta(s)/\delta(s) = K_o/s^2 \quad (K_o = 11.7 \text{ deg.-sec.}^{-2}/\text{deg.})$$

The command signal θ_c is filtered white noise w, with the filter :

$$\theta_c(s)/w(s) = 3.67/(s^2 + 3s + 2.25)$$

and

$$E(w) = 0 \quad E[w(t)w(t+\sigma)] = \delta(\sigma)$$

With the tracking error defined as e = θ - θ_c, it is now assumed that the error signal is displayed to the pilot on a "fast" display, with first order lag at 50 rads/sec, i.e.

$$x_d(s) = \frac{50}{(s+50)} e(s)$$

The pilot's observations are the displayed variable x_d (in.) (and its associated rate ẋ_d) and his objective is to regulate the display signal to the best of his abilities. This task is reflected as that of minimizing the following performance index

$$J_p = E\{\lim_{T \rightarrow \infty} \frac{1}{T} \int_0^T (x_d^2 + g_p \dot{x}_d^2) dt\} \quad (1)$$

where g_p may be chosen to yield a neuromuscular lag time constant, for example, τ_n = 0.1 seconds.

For all the analysis results presented here, the following values were used for the parameters in the OCM :

- (1) Pilot is assumed to reconstruct the rate information from the displayed variable, thus attention allocation is 1 for both the observations x_d and ẋ_d.

(11) Observation thresholds for x_d and \dot{x}_d were 0.012 in. and 0.036 in./sec. respectively based on visual arc angles of 0.05 deg. and 0.15 deg./sec. at the pilot's eye and assuming the display to be 1 ft. away from the pilot's eye.

(111) Observation noise ratio of -20 dB for each observation.

(iv) Motor noise ratio of -20 dB.

(v) Observation time delay, $\tau=0.1$ seconds.

The predicted 'piloted' system performance for the augmented plant is given in Table I. (Note that these results differ from those in Ref. [6] because of the different thresholds and attention allocation for the display considered).

Table I. Unaugmented System Performance

g_p	e rms (deg)	δ rms (deg)	$\dot{\delta}$ rms (deg/sec)	J_p
0.009	0.812	0.802	5.95	0.98

The results in Table I. are indicative of high levels of tracking error and pilot workload. We then wish to improve tracking performance and reduce pilot workload by a suitable choice of display and/or control augmentation using only θ feedback as shown in the block diagram of Fig. 2. The use of only rate feedback is consistent with the previous discussion. Note that with display augmentation, the signal being observed (and regulated) by the pilot is :

$$x_d(s) = \frac{50}{(s+50)} (e - K_d \dot{\theta})$$

and is no longer just lagged error.

Within the framework of the Cooperative Display/Control design methodology, the form of augmentation shown in Fig. 2 leads to the following definitions :

$$\bar{y}_1 = [x_d, \dot{x}_d]' + \bar{v}_y ; \bar{y}_2 = [\dot{\theta}, \delta]' ; y_d = \dot{\theta}$$

$$G_2 = [-K_c, K_\delta] ; G_d = -K_d$$

$$J_1 = J_p \quad (\text{with } J_p \text{ as in Eqn. (1)})$$

The choice of the cost function J_2 should reflect the various tradeoffs that are involved in the design of the augmentation. For the results presented herein, J_2 was chosen to be

$$J_2 = E \left\{ \lim_{T \rightarrow \infty} \frac{1}{T} \int_0^T (e^2 + g \delta_p^2 + F_2 u_2^2 + F_{2d} u_d^2) dt \right\}$$

with $g=0.009$ (corresponding to g_p for the unaugmented case, as in Table I.). Wierwille et al. [16] have shown that the pilot's perception of workload is strongly correlated with the rms value of his control input rate, so the inclusion of $\dot{\delta}$ in the cost function J_2 reflects the desire to minimize pilot workload. Clearly the inclusion of error reflects the desire to provide good tracking

performance. The weights F_2 and F_{2d} (scalars for this cost) control the levels of augmentation control energy and "display energy", respectively, being introduced into the system. For $F_2 = F_{2d} = 0$, J_2 equals J_p .

Using the Cooperative methodology, four different cases of augmentation were considered. These cases are discussed below.

A. Display Augmentation only

The results of display augmentation synthesis, without augmenting plant dynamics, for varying F_{2d} are listed in Table II. along with the evaluation results using the full-order model. As is to be expected, the value of K_d increases as F_{2d} is decreased, but interestingly K_d reaches a

limiting value of 0.373 in./deg.-sec.⁻¹ as $F_{2d} \rightarrow 0$. Note that this limiting value is very close to the value of K_d obtained earlier for minimum pilot workload using the cross-over model. The fact that it is slightly lower than the value 0.4 can be attributed in part to the lower value of the pilot's observation time delay used in the synthesis procedure and that error was not a primary design objective in the classical approach. Thus as the allowable level of "display energy" into the system is increased, the methodology leads to a design that meets the pilot-centered requirements. The results of Table II. are also plotted in Fig. 3 and Fig. 4. Fig. 3 is a plot of rms error (e) vs. rms manual control rate ($\dot{\delta}_p$), and Fig. 4 is a plot of rms error vs.

total control activity (δ) acting on the plant. It is clear from these two figures that the pilot's workload (of which $\dot{\delta}_p$ is a measure) and the total control activity decrease monotonically as the display augmentation gain K_d is increased. The rms error initially decreases as K_d is increased, but then starts increasing beyond a certain value of K_d . The limiting value corresponds to the case beyond which increasing K_d will lead to much degraded performance without any significant reduction in pilot workload. If the pilot's performance index J_p is used to predict the pilot

opinion rating [11,17], then the results in Table II. also indicate that there will be no further improvement in pilot opinion rating for increasing K_d beyond the limiting value.

B. Control Augmentation Only

The results for control augmentation synthesis alone (without display augmentation), are listed in Table III., along with the evaluation results using the full-order OCM pilot model. Again it is noted that as $F_2 \rightarrow 0$, the limiting value of $K_c = 0.62$ deg./deg.-sec.⁻¹ that is achieved, corresponds to $K_{oc} = 7.2$ which is quite close to the value obtained earlier using the cross-over model with the minimum-pilot-workload objective. Thus as the allowable level of control energy into the system is increased the methodology leads to a design that again meets the pilot-centered requirements. The results of Table III. are also plotted in Figs. 3 and 4. These results indicate that the tracking performance improves monotonically as the level of control

augmentation is increased and the pilot workload also reduces. However, the total control activity acting on the plant (δ) starts increasing beyond a certain value of K_d . A good intermediate value of K_d might correspond to that value beyond which very high levels of total control deflection result, with negligible improvement in tracking performance and no noticeable reduction in pilot workload.

Comparing the results for display augmentation alone with those for control augmentation alone, it is evident that control augmentation has the advantage of significantly improving tracking performance, while display augmentation has the advantage of significantly reducing pilot workload and total control deflection. This leads one to conjecture that even for the simple k/s^2 plant, there might be some advantage to providing a combination of control and display augmentation as opposed to control augmentation alone or display augmentation alone.

C. Display Design for Control Augmented Plants

For four of the control-augmented plants above, a display-augmentation synthesis was carried out, using the same cost index J_2 as before. As the level of display augmentation was increased (F_{2d} was decreased) for a given control-augmented plant, the same behavior was observed as in the case of display design for the unaugmented plant, i.e. the error first decreased and then started increasing while there was continuous reduction in pilot workload (δ_p) and total control activity (δ). As with the K_o/s^2 plant case, the error was found to be the least for the choice of $F_{2d}=1$ for all the control augmented plants. The synthesis results and the predicted performance corresponding to the "best" choice of weighting on the display controller (i.e. $F_{2d}=1$) are listed in Table IV. These results are also plotted in Figs. 3 and 4.

It is interesting to note from Table IV. that as the plant itself becomes more and more like k/s (or as K is increased), the required level of display augmentation decreases - even though the performance index being minimized (J_2) is the same in all cases. This is an indication of the interdependence between control and display augmentation for any given task. Also, the synthesized display augmentation is such that the pilot workload (δ_p) is roughly the same for all the cases presented in Table IV. This result is in agreement with the findings in Ref. [2] that the pilot workload tends to be constant for specific combinations of control and display sophistication.

D. Simultaneous Control/Display Synthesis

For the same cost weightings (F_2 and F_{2d}) considered above, the cooperative synthesis algorithm was again exercised except now the simultaneous synthesis of the control and display augmentation gains G_c and G_d was performed. The synthesis results and the predicted closed-loop performance are listed in Table V. Again, as the level of control augmentation is increased, the

F_{2d}	K_d	e_{rms} (deg)	δ_{rms} (deg)	$\dot{\delta}_{rms}$ (deg/sec)	J_P
10	0.032	0.756	0.749	5.58	0.82
1	0.230	0.623	0.453	3.38	0.41
0.1	0.353	0.634	0.345	2.56	0.35
0.01	0.373	0.638	0.333	2.46	0.34
0.001	0.373	0.638	0.333	2.46	0.34

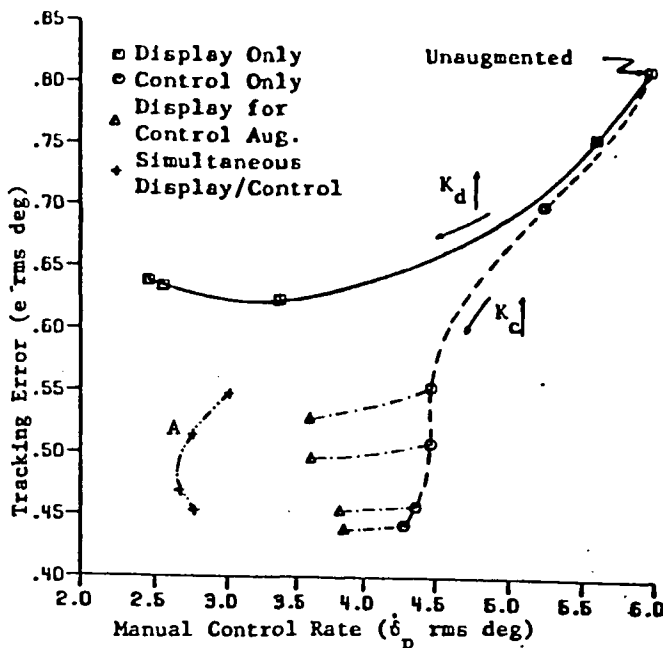


Fig. 3 Performance and Workload Comparison

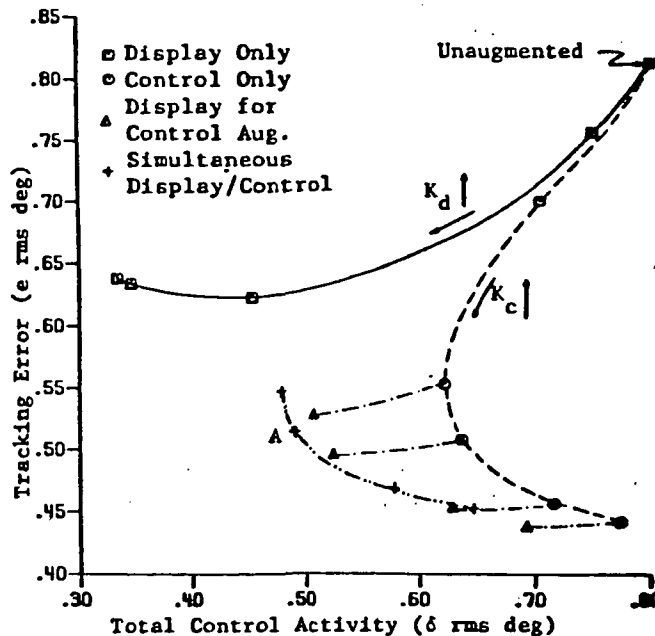


Fig. 4 Performance and Total Control Activity Comparison

F_2	K_c (deg/deg-sec ⁻¹)	K_δ	e rms (deg)	δ rms (deg)	$\dot{\delta}$ rms (deg/sec)	J_P
10	0.029	0.020	0.700	0.704	5.22	0.70
2	0.116	0.149	0.553	0.622	4.46	0.42
1	0.203	0.285	0.508	0.637	4.46	0.35
0.33	0.461	0.841	0.457	0.716	4.36	0.28
0.1	0.617	1.276	0.442	0.774	4.28	0.26
0.01	0.620	1.284	0.442	0.774	4.28	0.26

Table IV. Display Design for Control-Augmented Plants

$$(F_{2d} = 1)$$

K_c (deg/deg-sec ⁻¹)	K_δ	K_d (in/deg-sec ⁻¹)	e rms (deg)	δ rms (deg)	$\dot{\delta}$ rms (deg/sec)	J_P
0.116	0.149	0.123	0.528	0.507	3.61	0.28
0.203	0.285	0.116	0.496	0.525	3.62	0.24
0.461	0.841	0.095	0.454	0.629	3.83	0.21
0.617	1.276	0.087	0.439	0.693	3.86	0.20

Table V. Simultaneous Display/Control Design

$$(F_{2d} = 1)$$

F_2	K_c (deg/deg-sec ⁻¹)	K_δ	K_d (in/deg-sec ⁻¹)	e rms (deg)	δ rms (deg)	$\dot{\delta}$ rms (deg/sec)	J_P
2	0.082	0.260	0.153	0.547	0.479	3.02	0.29
1	0.144	0.498	0.132	0.514	0.490	2.76	0.26
0.33	0.344	1.198	0.108	0.469	0.578	2.67	0.22
0.1	0.437	1.576	0.076	0.453	0.647	2.77	0.22

level of display augmentation decreases. The results of Table V. are also plotted in Figs. 3 and 4. Comparing these results to those of Section IV C. above, we note that for the same level of closed-loop performance (e rms), the total control activity (δ) is roughly the same in both cases, but the pilot's control input rate ($\dot{\delta}$) is lower for the case of simultaneous synthesis. This is true even when the results are compared for the same level of plant augmentation (K). This can be shown by simply cross-plotting the above results versus K_c .

A candidate design that offers improvement in all aspects over the unaugmented case is the one obtained by simultaneous display/control synthesis with the weights of $F_2=1$ and $F_{2d}=1$ (see Table V.). From Figs. 3 and 4 we note that for this case (labelled A in the figures), the tracking performance is much improved over the unaugmented

case, the total control activity is much lower, the pilot's control input rate is much reduced and the level of control augmentation (K) is not too high. The frequency responses of the effective controlled element ($x_d/\delta(j\omega)$) for the candidate design and the unaugmented plant are compared in Fig. 5. The candidate design is close to k/s over a broad frequency region. (As stated earlier, the effective controlled element can be made exactly like k/s by increasing the values of the gains K and K_d , but doing the former will have the effect of increasing the required total control deflection, while doing the latter will result in degraded tracking performance). The predicted pilot describing function ($P(j\omega)$) for the candidate design and the unaugmented plant are compared in Fig. 6, and the resulting loop frequency responses $P(j\omega) \cdot x_d/\delta(j\omega)$ are shown in Fig. 7. The cross-over frequency (ω_c), the gain

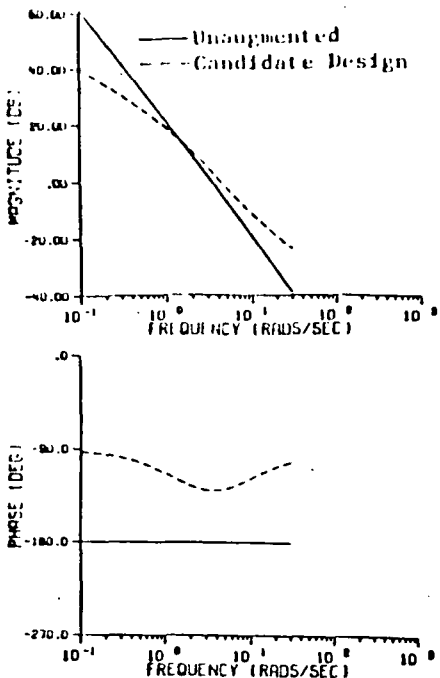


Fig. 5 Effective Controlled Element ($x_d/\delta_p(j\omega)$)

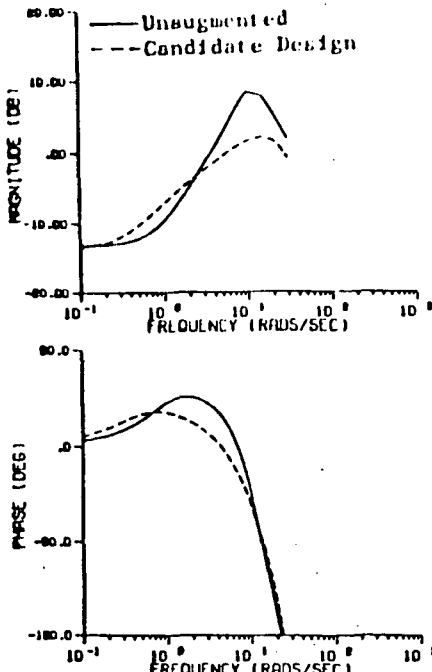


Fig. 6 Pilot Describing Function ($P(j\omega)$)

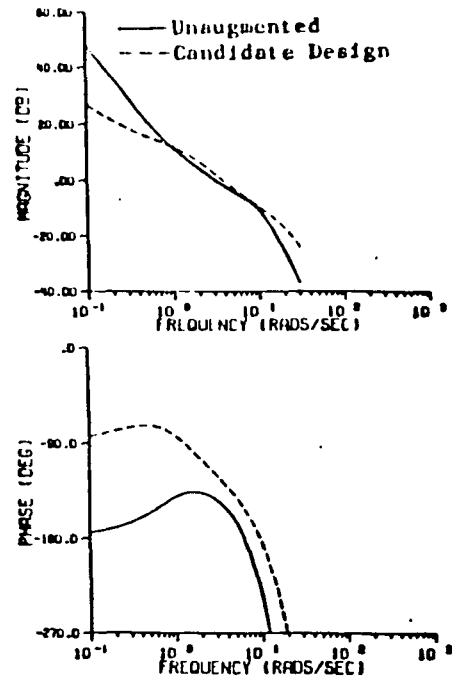


Fig. 7 Loop Transfer Function ($P(j\omega) \cdot x_d/\delta_p(j\omega)$)

margin (G.M.), and phase margin (P.M.) obtained from Fig. 7 are noted in Table VI. We note that for the candidate design, not only is the cross-over frequency higher, but also the stability margins are much improved over the unaugmented case. Going back to Fig. 6, we note that for the candidate design the pilot's phase compensation is much lower than for the unaugmented case. The pilot's phase compensation at cross-over, with the effect of the neuro-muscular lag and the observation time delay removed^[18] (ζ pc) is also listed in Table VI.

Table VI. Frequency-domain Comparison

Controlled Element	G.M. (dB)	P.M. (deg)	ω (rads/sec)	ζ pc (deg)
Unaugmented	6.0	26	3.1	75
Candidate Design	9.0	50	3.9	47

V. CONCLUSIONS

A methodology was presented that has the potential of providing a task-specific, systematic trade-off between control and display augmentation, taking into account the limits of the human pilot as an "information processor and controller". Various control and display augmentation laws were synthesized using the methodology for a compensatory tracking task with a k/s^2 plant. Analytical evaluations of the synthesized laws demonstrate the applicability of the methodology to meet the pilot-centered requirements for display design. The results also indicate that simultaneous control/display synthesis leads to a better design, as opposed to

designing the display after the control laws have been designed.

Further theoretical work needs to be done in terms of the asymptotic properties of the synthesis methodology and the numerical properties of the solution algorithm - although no numerical problems were encountered. Finally, experimental validation is warranted.

ACKNOWLEDGEMENT

This research was supported by NASA Dryden Flight Research Facility, Ames Research Center under grants NAG2-228 and NAG4-1. Mr. E. L. Duke and Mr. Donald T. Berry are the technical monitors, respectively. This support is gratefully appreciated.

APPENDIX

OPTIMAL COOPERATIVE CONTROL/DISPLAY DESIGN METHODOLOGY

Problem Formulation

Consider a dynamic system acted upon by two controllers, and described by the linear time invariant set of first order differential equations

$$\dot{\bar{x}} = A_0 \bar{x} + B_{10} \bar{u}_1 + B_{20} \bar{u}_2 + D_0 \bar{w} \quad (A.1)$$

with $\bar{x} \in R^n$, $\bar{u}_1 \in R^{m_1}$, $\bar{u}_2 \in R^{m_2}$ and \bar{w} a zero-mean Gaussian white noise process with intensity W . The two controls represent two physically independent controllers.

The display dynamics are assumed to be of the form

$$\dot{\bar{x}}_d = A_d \bar{x}_d + B_{do} \bar{u}_d \quad (A.2)$$

with $\bar{x}_d \in R^d$, $\bar{u}_d \in R^m$, where \bar{u}_d is the display "quickening" Controller. The objective is to find the optimal cooperative controllers 1 and 2 (\bar{u}_1 and \bar{u}_2) along with the optimal display control law \bar{u}_d .

Controller 1 (\bar{u}_1) is assumed to have noisy observations available for feedback given by

$$\bar{y}_1 = C_{1o} \bar{x} + C_{d1} \bar{x}_d + C_u \bar{u}_d + \bar{v}_y \quad (A.3)$$

where \bar{v}_y is also a zero-mean Gaussian white noise process with intensity V . This controller will have the form of an LQG compensator, i.e. it consists of full state feedback implemented using a Kalman estimator.

The augmentation controller \bar{u}_2 and the display control law \bar{u}_d are assumed to have noise-free measurements \bar{y}_2 and \bar{y}_d , respectively, available for feedback, where

$$\bar{y}_2 = C_{2o} \bar{x}; \quad \bar{y}_d = C_d \begin{bmatrix} \bar{x} \\ \bar{x}_d \end{bmatrix} \quad (A.4)$$

Note that the above formulation does not allow feedback of the display states \bar{x}_d to the augmentation controller \bar{u}_2 . Finally, these two latter controllers are constrained to have the direct output feedback form

$$\begin{aligned} \bar{u}_2 &= G_2 \bar{y}_2 = G_2 C_{2o} \bar{x} \\ \bar{u}_d &= G_d \bar{y}_d = G_d C_d \begin{bmatrix} \bar{x} \\ \bar{x}_d \end{bmatrix} \end{aligned} \quad (A.5)$$

The interaction between the different controllers is shown in the block diagram of Fig. A.1

Design Objectives

Controller 1 is to be optimal with respect to the cost

$$J_1 = E \left\{ \lim_{T \rightarrow \infty} \frac{1}{T} \int_0^T (\bar{x}^T Q_{1o} \bar{x} + \bar{x}_d^T Q_{1d} \bar{x}_d + \bar{u}_1^T R_1 \bar{u}_1 + \bar{u}_2^T F_1 \bar{u}_2) dt \right\} \quad (A.6)$$

in the presence of the action of control inputs \bar{u}_2 and \bar{u}_d . Here $E\{\cdot\}$ indicates the expected value operator and the weighting matrices are $Q_{1o} > 0$, $Q_{1d} > 0$, $R_1 > 0$, $F_1 > 0$. Conversely, Controller 2 (\bar{u}_2) and the display control law \bar{u}_d are to be optimal with respect to the cost

$$J_2 = E \left\{ \lim_{t \rightarrow \infty} \frac{1}{T} \int_0^T (\bar{x}^T Q_{2o} \bar{x} + \bar{x}_d^T Q_{2d} \bar{x}_d + \bar{u}_2^T R_2 \bar{u}_2 + \bar{u}_d^T F_2 \bar{u}_d + \bar{u}_d^T F_{2d} \bar{u}_d) dt \right\} \quad (A.7)$$

in the presence of the control action \bar{u}_1 . The weighting matrices are $Q_{2o} > 0$, $Q_{2d} > 0$, $R_2 > 0$, $F_2 > 0$, $F_{2d} > 0$.

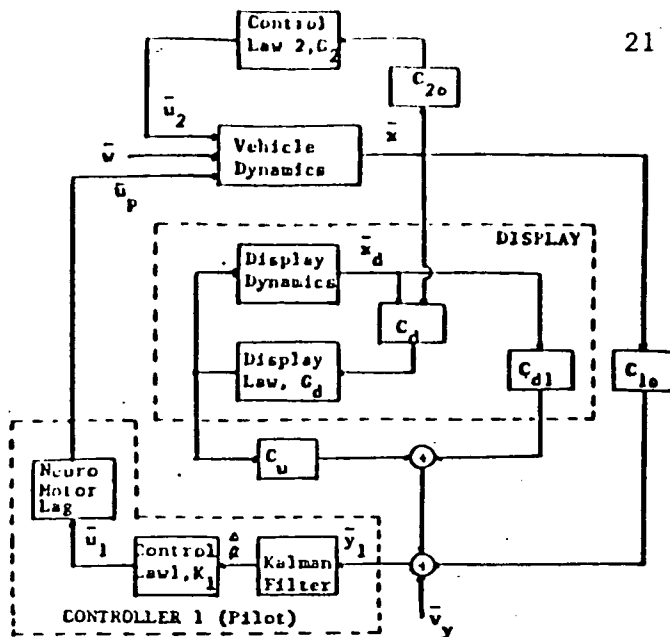


Fig. A.1 Block Diagram for Cooperative Control/Display Augmentation

Augmenting the system dynamics (A.1) with the display dynamics (A.2), the state-space description of this augmented system is

$$\begin{bmatrix} \dot{\bar{x}} \\ \dot{\bar{x}}_d \end{bmatrix} = \begin{bmatrix} A_o & 0 \\ 0 & A_d \end{bmatrix} \begin{bmatrix} \bar{x} \\ \bar{x}_d \end{bmatrix} + \begin{bmatrix} B_{1o} \\ 0 \end{bmatrix} \bar{u}_1 + \begin{bmatrix} B_{2o} \\ 0 \end{bmatrix} \bar{u}_2 + \begin{bmatrix} 0 \\ B_{do} \end{bmatrix} \bar{u}_d + \begin{bmatrix} D_o \\ 0 \end{bmatrix} \bar{w} \quad (A.8)$$

Defining $\bar{x} = \text{COL}(\bar{x}, \bar{x}_d)$, (A.8) can be written in a compact form with appropriate definitions for the matrices as

$$\dot{\bar{x}} = A \bar{x} + B_1 \bar{u}_1 + B_2 \bar{u}_2 + B_d \bar{u}_d + D \bar{w} \quad (A.9)$$

The measurements can similarly be written as

$$\begin{aligned} \bar{y}_1 &= C_1 \bar{x} + C_u \bar{u}_d + \bar{v}_y \\ \bar{y}_2 &= C_2 \bar{x} \\ \bar{y}_d &= C_d \bar{x} \end{aligned} \quad (A.10)$$

The two cost functions can then be expressed in terms of the augmented state vector \bar{x} as

$$\begin{aligned} J_1 &= E \left\{ \lim_{T \rightarrow \infty} \frac{1}{T} \int_0^T (\bar{x}^T Q_1 \bar{x} + \bar{u}_1^T R_1 \bar{u}_1 + \bar{u}_2^T F_1 \bar{u}_2) dt \right\} \\ J_2 &= E \left\{ \lim_{T \rightarrow \infty} \frac{1}{T} \int_0^T (\bar{x}^T Q_2 \bar{x} + \bar{u}_1^T R_2 \bar{u}_1 + \bar{u}_2^T F_2 \bar{u}_2 + \bar{u}_d^T F_{2d} \bar{u}_d) dt \right\} \end{aligned} \quad (A.11)$$

where the weighting matrices Q_1 and Q_2 are appropriately defined. Note that this formulation

is formally that for a multi-player non-zero sum game, and we seek a Nash solution [19].

Solution for \bar{u}_1

In the presence of the action of control inputs \bar{u}_2 and \bar{u}_d , as given by (A.5), the dynamics of the augmented system (A.9) are

$$\begin{aligned} \dot{\bar{X}} &= A_{aug} \bar{X} + B_1 \bar{u}_1 + D \bar{w} \\ \bar{y}_1 &= C_{aug} \bar{X} + \bar{v}_y \end{aligned} \quad (A.12)$$

where

$$\begin{aligned} A_{aug} &\triangleq (A + B_2 C_2 C_2 + B_d G_d C_d) \\ C_{aug} &\triangleq (C_1 + C_u G_d C_d) \end{aligned} \quad (A.13)$$

and the performance index J_1 becomes

$$J_1 = E \left\{ \lim_{T \rightarrow \infty} \frac{1}{T} \int_0^T (\bar{X}^T (Q_1 + C_2^T C_2^T F_1 C_2 C_2) \bar{X} + \bar{u}_1^T R_1 \bar{u}_1) dt \right\} \quad (A.14)$$

Equations (A.12) and (A.14), in the case of uncorrelated process and measurement noises (\bar{w} and \bar{v}) and for $V > 0$ (i.e. V - positive definite), describe the standard non-singular linear quadratic Gaussian regulator problem for controller \bar{u}_1 . The optimal controller is known [20] to have the form

$$\bar{u}_1 = K_1 \hat{\bar{X}} \quad (A.15)$$

where $\hat{\bar{X}}$ is the minimum mean-square estimate of the system state vector \bar{X} . The gain matrix K_1 is given by

$$K_1 = -R_1^{-1} B_1^T P \quad (A.16)$$

with $P > 0$ and symmetric, the solution of the algebraic Riccati equation

$$A_{aug}^T P + P A_{aug} + (Q_1 + C_2^T C_2^T F_1 C_2 C_2) - P B_1^T R_1^{-1} B_1 P = 0 \quad (A.17)$$

The dynamics of the Kalman state estimator are

$$\dot{\hat{\bar{X}}} = A_{aug} \hat{\bar{X}} + B_1 \bar{u}_1 + M_1 (\bar{y}_1 - C_{aug} \hat{\bar{X}}) \quad (A.18)$$

where the Kalman filter gain matrix M_1 is given by

$$M_1 = \Gamma C_{aug}^T V^{-1} \quad (A.19)$$

with $\Gamma (> 0)$ the solution of the algebraic Riccati equation

$$\begin{aligned} A_{aug} \Gamma + \Gamma A_{aug}^T + D W D^T - \Gamma C_{aug}^T V^{-1} C_{aug} \Gamma &= 0 \end{aligned} \quad (A.20)$$

Solution for \bar{u}_2 and \bar{u}_d

The optimal controller \bar{u}_1 as derived above

has the form

$$\bar{u}_1 = K_1 \hat{\bar{X}}; \quad \dot{\hat{\bar{X}}} = A_1 \hat{\bar{X}} + M_1 \bar{y}_1 \quad (A.21)$$

where $A_1 \triangleq (A_{aug} + B_1 K_1 - M_1 C_{aug})$. Then in the presence of this control action \bar{u}_1 , the system dynamics (A.9, A.15, A.18) can be written in terms of the augmented state vector $\bar{q} \triangleq \text{COL}(\bar{X}, \hat{\bar{X}})$ as

$$\dot{\bar{q}} = \begin{bmatrix} A & B_1 K_1 \\ M_1 C_1 & A_1 \end{bmatrix} \bar{q} + \begin{bmatrix} B_2 \\ 0 \end{bmatrix} \bar{u}_2 + \begin{bmatrix} B_d \\ 0 \\ 0 \\ M_1 C_u \end{bmatrix} \bar{u}_d + \begin{bmatrix} D & 0 \\ 0 & M_1 \end{bmatrix} \begin{bmatrix} \bar{w} \\ \bar{v}_y \end{bmatrix} \quad (A.22)$$

which can further be written in a compact form, with appropriate definitions of matrices, as

$$\dot{\bar{q}} = A_1' \bar{q} + B_2' \bar{u}_2 + B_d' \bar{u}_d + D' \bar{w}' \quad (A.23)$$

The intensity of the process \bar{w}' is $W' = \begin{bmatrix} W & 0 \\ 0 & V \end{bmatrix}$.

The index of performance to be minimized by \bar{u}_2 and \bar{u}_d then becomes

$$J_2 = E \left\{ \lim_{T \rightarrow \infty} \frac{1}{T} \int_0^T (\bar{q}^T Q' \bar{q} + \bar{u}_2^T F_2 \bar{u}_2 + \bar{u}_d^T F_{2d} \bar{u}_d) dt \right\} \quad (A.24)$$

with

$$Q' \triangleq \begin{bmatrix} Q_2 & 0 \\ 0 & K_1^T R_2 K_1 \end{bmatrix}$$

The design objective can then be stated as that of finding the optimal controller \bar{u}_2 and optimal display control \bar{u}_d which minimize the cost J_2 as given by (A.24), subject to (A.23).

It can be shown [8] that the gains G_2 and G_d which correspond to the simultaneous optimality of the two controllers \bar{u}_2 and \bar{u}_d are given by

$$G_2 = -F_2^{-1} [B_2^T \ 0] \text{HL} \begin{bmatrix} C_2^T \\ 0 \end{bmatrix} \left([C_2 \ 0] L \begin{bmatrix} C_2^T \\ 0 \end{bmatrix} \right)^{-1} \quad (A.25)$$

and

$$G_d = -F_{2d}^{-1} \begin{bmatrix} B_d^T \\ M_1 C_u \end{bmatrix}^T \text{HL} \begin{bmatrix} C_d^T \\ 0 \end{bmatrix} \left([C_d \ 0] L \begin{bmatrix} C_d^T \\ 0 \end{bmatrix} \right)^{-1} \quad (A.26)$$

Here, $L = E\{\bar{q} \bar{q}^T\}$ satisfies the relation

$$A_c L + L A_c^T + D' W' D'^T = 0 \quad (A.27)$$

and H satisfies

$$A_c^T H + H A_c + \bar{Q} = 0 \quad (A.28)$$

where the following definitions have been used

$$\bar{Q} = \frac{\Delta}{Q'} + \begin{bmatrix} A_{aug} & B_1 K_1 \\ M_1 C_{aug} & A_1 \\ C_2^T G_2^T F_2 G_2 C_2 + C_d^T G_d^T F_d G_d C_d & 0 \\ 0 & 0 \end{bmatrix}$$

The solutions (A.25) and (A.26) are derived from the gradient conditions

$$\frac{\partial \bar{J}_2}{\partial C_2} = 2(F_2 G_2 [C_2 \ 0] L \begin{bmatrix} C_2^T \\ 0 \end{bmatrix}) + \quad (A.29)$$

$$[B_2^T \ 0] H L \begin{bmatrix} C_2^T \\ 0 \end{bmatrix} = 0$$

and

$$\frac{\partial \bar{J}_2}{\partial G_d} = 2(F_d G_d [C_d \ 0] L \begin{bmatrix} C_d^T \\ 0 \end{bmatrix}) + \quad (A.30)$$

$$\begin{bmatrix} B_d \\ M_1 C_u \end{bmatrix}^T H L \begin{bmatrix} C_d^T \\ 0 \end{bmatrix} = 0$$

respectively.

Thus the solution to cooperative control/display synthesis problem requires simultaneously solving two Algebraic Riccati equations (Eqn. (A.17) for the control gains for Controller 1 and (A.20) for the estimator gains), two Lyapunov equations (Eqn. (A.27) for the system covariance matrix and (A.28) for the matrix of Lagrange multipliers) and two gradient conditions (Eqns. (A.29) and (A.30)) which are necessary for the optimality of the gains G_2 and G_d . A computer program using a conjugate gradient search algorithm with cubic interpolation [21] was developed to solve for the optimal augmentation gains.

REFERENCES

- [1] "V/STOL Displays for Approach and Landing," AGARD Rep. No. 594, 1972.
- [2] Lebacqz, J.V., Gerdes, R.M., Forrest, R.D., and Merrill, R.K., "Investigation of Control, Display, and Crew-Loading Requirements for Helicopter Instrument Approach," Journal of Guidance and Control, Vol. 4, No. 6, Nov.-Dec. 1981, pp. 614-622.
- [3] Lebacqz, J.V., "Ground Simulation Investigation of Helicopter Decelerating Instrument Approaches," Journal of Guidance and Control, Vol. 6, No. 5, Sept.-Oct. 1983, pp. 330-338.
- [4] Duke, E.L., Jones, F.P., and Roncoli, R.B.,

"Development of a Flight Test Maneuver Autopilot for a Highly Maneuverable Aircraft," AIAA Paper 83-0061, Jan. 1983. 23

- [5] Duke, E.L., Swann, M.R., Enevoldson, E.K., and Wolf, T.D., "Experience with Flight Test Trajectory Guidance," Journal of Guidance and Control, Vol. 6, No. 5, Sept.-Oct. 1983, pp. 393-398.
- [6] Schmidt, D.K., "Optimal Flight Control Synthesis via Pilot Modeling," Journal of Guidance and Control, Vol. 2, No. 4, July-Aug. 1979, pp. 308-312.
- [7] Schmidt, D.K., and Innocenti, M., "Optimal Cooperative Control Applied to a Control Configured Aircraft," NASA CR-170411, Jan. 1984.
- [8] Garg, S., and Schmidt, D.K., "Optimal Cooperative Control Synthesis of Active Displays," Final Report for grant NAG2-228, submitted to NASA Dryden Flight Research Facility, Ames Research Center, 22nd Oct. 1985.
- [9] Kleinman, D.R., Baron, S., and Levison, W.H., "An Optimal Control Model of Human Response," Parts I and II, Automatica, Vol. 6, pp. 357-383, 1970.
- [10] Levison, W.H., "A Model-Based Technique for the Design of Flight Directors," Proceedings of the Ninth Annual Conference on Manual Control, May 1973, pp. 163-172.
- [11] Hess, R.A., "Analytical Display Design for Flight Tasks conducted under Instrument Meteorological Conditions," NASA TM X-73,146, August 1976.
- [12] Hoffman, W.C., Kleinman, D.L., and Young, L.R., "Display/Control Requirements for Automated VTOL Aircraft," NASA CR-158905, ASI-TR-76-39, October 1976.
- [13] Weir, D.H., Klein, R.H., and McRuer, D.T., "Principles for the Design of Advanced Flight Director Systems Based on the Theory of Manual Control Displays," NASA CR-1748, March 1971.
- [14] McRuer, D.T., and Jex, H.R., "A Review of Quasi-Linear Pilot Models," Transactions on Human Factors in Electronics, Vol. HFE-8, No. 3, Sept. 1967, pp. 231-249.
- [15] Phatak, Anil V., "Investigation of Alternate Human Operator Optimal Control Structures," Air Force RMRL, Contract # F33615-78-C-0501.
- [16] Wierwille, W.W., and Connor, S.A., "Evaluation of 20 Workload Measures Using a Psychomotor Task in a Moving-Base Aircraft Simulator," Human Factors, Vol. 25, pp. 1-16, 1983.
- [17] Schmidt, D.K., "On the Use of the OCM's Objective Function as a Pilot Rating Metric," Proceedings of 17th Annual Conference on Manual Control, Los Angeles, Calif., June 1981.

- [18] Bacon, B.J., and Schmidt, D.K., "An Optimal Control Approach to Pilot/Vehicle Analysis and the Neal-Smith Criteria," *Journal of Guidance and Control*, Vol. 6, No. 5, Sept.-Oct. 1983, pp. 339-347.
- [19] Pavasilopoulos, G.P., Medanic, J.V., Cruz, J.B. Jr., "On the Existence of Nash Strategies and Solutions to Coupled Riccati equations in Linear-Quadratic Games," *Journal of Optimization Theory and Applications*, Vol. 28, No. 1, May 1979.
- [20] Kwakernaak, H., and Sivan, R., "Linear Optimal Control Systems," Wiley-Interscience, 1972.
- [21] Fletcher, R., and Powell, M.J.D., "A Rapidly Convergent Descent Method for Minimization," *Computer Journal*, Vol. 6, pp. 163-168, 1963.

ORIGINAL PAGE IS
OF POOR QUALITY